Revisions to the ASTER temperature /emissivity separation algorithm

William T. Gustafson, Alan R. Gillespie, Gail J. Yamada
Keck Spectral Remote Sensing Lab,
Department of Earth and Space Sciences, University of Washington

ABSTRACT

ABSTRACT - ***The ASTER temperature/emissivity separation (TES) algorithm is used to make Standard Products containing surface temperature and emissivity images. It operates on land-leaving TIR radiance products, corrected for atmospheric transmissivity and sky radiance. Uncertainties were attributed to 1) calibration, 2) atmospheric correction, and 3) measurement errors. Uncertainty is also introduced by an empirical power-law regression used to scale ASTER emissivity spectra. The 1-σ accuracy and precision were estimated at 1.5 K and 0.015, respectively, from models before the December 1999 launch of Terra and validated by field experiments. Later, however, errors of 4 K and scaling errors in emissivity were encountered in some images, especially in areas of low spectral contrast. We have undertaken to assess the magnitude and cause of this problem, and to rectify it if possible. It appears that errors in calibration and atmospheric compensation have led to over-correction for reflected downwelling irradiance and unacceptable errors in emissivity scaling. Serious inaccuracies occurred in ~4-5% of all frames, especially those taken near the ocean and with high atmospheric temperatures and humidity. Calibration errors have recently been reduced. Changes in TES have also improved the appearance of ASTER Standard Products: iterative correction for downwelling irradiance and the threshold test for spectral contrast have been removed. Although inaccuracies related to calibration, atmospheric compensation, and the TES regression remain, exaggeration of those inaccuracies by the algorithm has been reduced significantly.***

INTRODUCTION

There are more unknowns than measurements in thermal-infrared remote sensing, and temperature and emissivity separation is an underdetermined inversion. The solution is only as good as the independent constraints that can be applied, together with the limitations imposed by measurement accuracy and precision. The independent constraints include atmospheric transmissivity and emission and, in the case of the ASTER temperature/emissivity separation (TES) algorithm, an empirical relationship between spectral emissivity (ε_a) contrast (Gillespie *et al.*, 1998). In this paper we evaluate the performance of the TES algorithm and propose changes to improve performance.

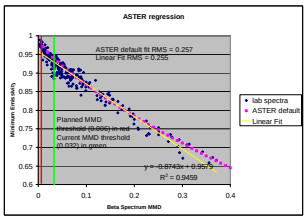

ASTER emin *vs.* MMD regressions, for 250 library spectra. "ASTER default" is the power-law curve used in TES. "Linear fit" is its replacement.

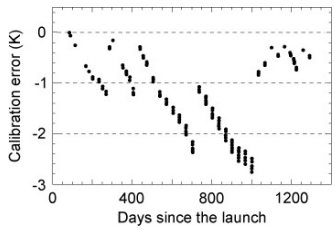

Calibration coefficients were updated frequently. For ASTER, when radiance errors reached the 1% level for any channel, all the calibration coefficients were recomputed. This caused a sawtoothed pattern over time in spectral radiance accuracies.

EXAMPLES

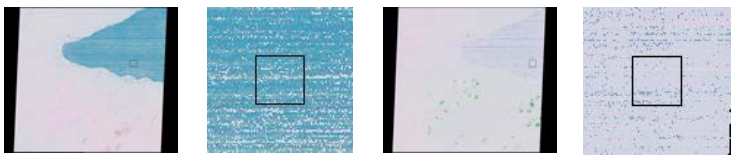

Lake Baikal error comparison. Both daytime images from southern part of Lake Baikal: R = 10, G = 12, B =14. Good scene 12 Aug 2004, 6% bad pixels; bad scene 22 Jul 2002, 89% bad pixels. Note clouds in the "good" picture.

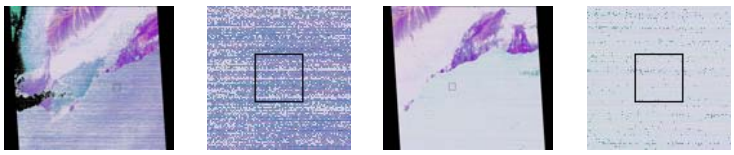

Hawaii error comparison. Both nighttime images from ocean south of the Big Island, Hawaii: R = 10, G = 12, B =14. Good scene 10 Jan 2004, 3% bad pixels; bad scene 02 Jun 2004, 76% bad pixels.

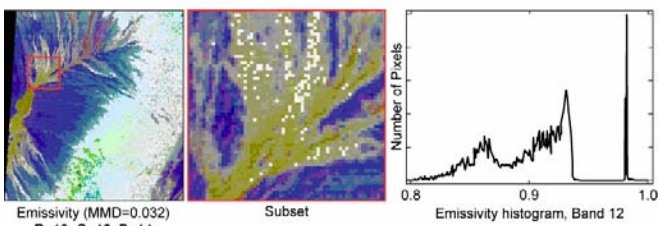

Spatial step discontinuities in a TES emissivity image (ASTER channel 12: 9.1 mm) of basalt flows on the island of Hawai'i with the MMD threshold value set to 0.032. a) Emissivity image. Rectangle is 64 90-m pixels (5.76 km) across. b) Subset from area of rectangle in *a*. c) Histogram of emissivities from the image subset. The gap and isolated spike in the histogram are due to the threshold test. In reality, the histogram should be continuous, with a tail out to 098. Because the emissivities are too high, temperatures are too low,
The step discontinuities are troubling because they disrupt the image for visual photo interpretation, they create local and unpredictable emissivity errors, and they create temperature errors. The last are especially troubling because many users are interested in water and canopy temperatures.

APPROACH

Gillespie *et al.* (1998) suggested that the principal sources of error in TES products were errors in 1) calibration, 2) atmospheric compensation, including correction for downwelling irradiance, 3) measurement errors, and 4) natural variability in the ε_{min} *vs.* MMD regression. In addition, of course, features of the algorithm itself, such as the successive estimation of the reflected downwelling term and the MMD threshold test, may contribute. In this assessment, we have examined calibration and atmospheric correction and their interactions with the TES code to explain the severity of the step discontinuities. We propose corrections to the algorithm and test them against the "problem" images to determine their effectiveness.

RESULTS

Scene	Lat	Lon	Elev. (m)	No.
Salton Sea	33N	116W	-69	5
Hawaii	19N	155W	0	20
Lake Baikal	52N	104E	444	7
Lake Tahoe	39N	120W	1901	57
Koko Nur	37N	100E	3193	5

Images of water used to estimate step-discontinuity error rates and test sensitivity to atmospheric compensation.

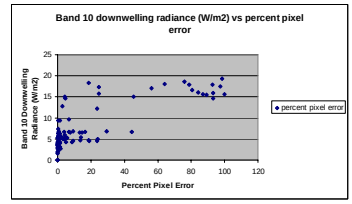

The percent error rate is shown above as a function of downwelling spectral irradiance, a measure of the magnitude of atmospheric correction. In general, the atmosphere above high-altitude lakes such as Koko Nur (Qinghai Lake) or Lake Tahoe can be expected to contain less water than above low-elevation lakes such as the Salton Sea.

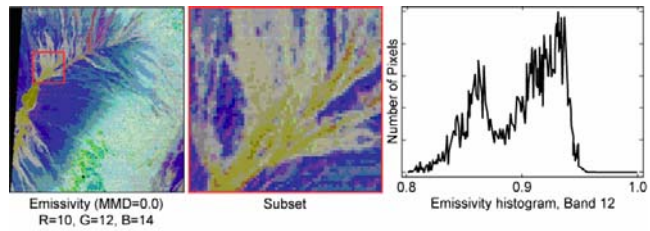

Step discontinuities affect only a small fraction of the images acquired by ASTER and the temperature and emissivity standard products. In the majority of instances, TES works properly, within the accuracies and precisions estimated by Gillespie *et al.* (1998). The remedies we propose for the step-discontinuity problem will improve the appearance of all images, but at the expense of decreased precision and accuracy over graybody scenes such as water.

RECOMMENDATIONS AND CONCLUSIONS

MMD threshold... The classification of pixels into categories of low- and high-contrast using the MMD threshold has proven unsatisfactory, and we have recommended removing it. This does not solve the underestimation problem, but at least does not increase the uncertainty. Figure 5 shows the improvement in appearance, and the change in the emissivity histogram, due to of this change on the Hawai'i image of Figure 2.
Irradiance correction... The iterative algorithm for the removal of spectral irradiance in TES fails frequently, probably due to inaccurate atmospheric correction, and should be eliminated.
In-scene atmospheric correction... It appears that the atmosphere transmissivity and emission are sufficiently changeable that accurate temperature/emissivity recovery requires that they be measured at the time of image acquisition. MODIS data have the potential to serve in this capacity, at least for specifying total column water on a near pixel-by-pixel basis. It may also be possible to adapt an approach such as ISAC (Young *et al.*, 2002) to increase the accuracy of the shape of the recovered emissivity spectrum, although application to complex scenes containing soils and rocks as well as graybodies and in any case accurate scaling of the emissivities requires independent scene classification such as used by the NDVI methods now (e.g., Sobrino *et al.*, 2001).
Temperatures for low-contrast scenes... Users interested in graybody (water, snow, or vegetation) temperatures *per se* should calculate it from Planck's Law using as inputs the spectral radiance data product (AST 9T) together with an assumed emissivity drawn for water, snow or vegetation from the ASTER spectral library. An independent separate classification of the scene using the VNIR bands or map data should be used to ensure that extracted temperatures are drawn from the correct material on the ground (Gustafson *et al.*, 2002).

BIBLIOGRAPHY

Abreu, L. W., F. X. Kneizys, G. P. Anderson, J. .H. Chetwynd, A. Berk, L. S. Bernstein, and D. C. Robertson, 1991. MODTRAN. *The Proceedings of the 1991 Battlefield Atmospheric Conference*, (El Paso, TX).
Anderson, G. P., J. H. Chetwynd, J.-M. Theriault, P. Acharya, A. Berk,, D. C. Robertson, F. X. Kneizys, M. L. Hoke, L. W. Abreu, and E. P. Shettle, 1993. MODTRAN2: Suitability for Remote Sensing. *The workshop on atmospheric correction of Landsat Imagery*. Edited by P. N. Slater, L. D. Mendenhall. (Torrance, CA: Geodynamix Corporation).
Fujisada. H. and A. Ono, Anticipated performance of ASTER instrument in EM design phase, *Proc. SPIE*, pp. 187-197, 1993.
Gesch, D.B., and K.S. Larson, 1996. Techniques for development of global 1-kilometer digital elevation models. *Pecora Thirteen, Human Interactions with the Environment-Perspectives from Space*, (Sioux Falls, SD)0, August 20-22, 1996.
Gillespie, A. R., 1987, Lithologic mapping of silicate rocks using TIMS data. *Proceedings of the. Workshop on Thermal Infrared Multispectral Scanner* held at the Jet Propulsion Laboratory, Pasadena, CA USA, 1987, Jet Propulsion Laboratory Publication 36-38, pp. 29-44.
Gillespie, A. R., Matsunaga, T., Rokugawa, S., and Hook, S. J., 1997, Temperature and Emissivity Separation from Advanced Spaceborne Thermal Emission and Reflection Radiometer (ASTER) Images. *IEEE Transactions on Geoscience and Remote Sensing*, 36, 1113-1126.
Gustafson, W. T., R. N. Handcock, A.R. Gillespie, and H. Tonooka, 2002. An image-sharpening method to recover stream tempoeratures from ASTEWR Images. SPIE Workshop: Remote Sensing for Environmental Monitoring, GIS Applications, and Geology II, Crete, Greece.
Kahle, A.B., F.D. Palluconi, S.J. Hook, V.J. Realmuto and G. Bothwell. 1991. The Advanced Spaceborne Thermal Emission and Reflectance Radiometer (ASTER). *International Journal of Imaging Systems and Technology*, 3: 144-156.
Kealy P. S. and S. Hook, 1993. Separating temperature and emissivity in thermal infrared multispectral scanner data: Implication for recovering land surface temperatures, *Trans. Geosci. Remote Sensing*, vol. 31, pp. 1155-1164.
Matsunaga, T. 1994. A temperature-emissivity separation method using an empirical relationship between the mean, the maximum, and the minimum of the thermal infrared emissivity spectrum, in Japanese with English abstract, *J. Rem. Sens. Soc. Japan*, vol. 14, no. 2, pp. 230-241.
Palluconi, F. D., G. Hoover, R. Alley and M. Jentoft-Nilsen, 1994. Atmospheric correction method for ASTER thermal radiometry over land, Algorithm Theoretical Basis Document, (Pasadena, CA: Jet Propulsion Laboratory).
Sobrino J. A, N. Raissouni, and Z.-L. Li, 2001. A comparative study of land surface emissivity retrieval from NOAA data *Remote Sensing of Environment* 2001; 75: 256-266.
Tonooka, H., F. Sakuma, and M. Kudoh, and K. Iwafune, 2003. ASTER/TIR onboard calibration status and user-based recalibration, *Proc. SPIE*, vol. 5234, pp. 191-201, 2003.
Yamaguchi, Y., H. Tsu and H. Fujisada, 1993. A scientific basis of ASTER instrument design, *SPIE Proc.*, pp. 150-160.
Young, S., B. Johnson, and J. Hackwell, 2002. An in-scene method for atmospheric compensation of thermal hyperspectral data, J. Geo. Res. 107(D24), pp. 1-14-20.